

Fidelity amplitude of the scattering matrix in microwave cavities

R Schäfer¹, T Gorin², T H Seligman³, and H-J Stöckmann¹

¹ Fachbereich Physik, Philipps-Universität Marburg, Renthof 5, D-35032 Marburg, Germany

² Max-Planck-Institut für Physik komplexer Systeme, Nöthnitzer Str. 38, D-01187 Dresden, Germany

³ Centro de Ciencias Físicas, Universidad Nacional Autónoma de México, Campus Morelos, C. P. 62251, Cuernavaca, Morelos, México

Abstract. The concept of fidelity decay is discussed from the point of view of the scattering matrix, and the *scattering fidelity* is introduced as the parametric cross-correlation of a given S-matrix element, taken in the time domain, normalized by the corresponding autocorrelation function. We show that for chaotic systems, this quantity represents the usual fidelity amplitude, if appropriate ensemble and/or energy averages are taken. We present a microwave experiment where the scattering fidelity is measured for an ensemble of chaotic systems. The results are in excellent agreement with random matrix theory for the standard fidelity amplitude. The only parameter, namely the perturbation strength could be determined independently from level dynamics of the system, thus providing a parameter free agreement between theory and experiment.

PACS numbers: 05.45.Mt, 03.65.Sq, 03.65.Yz

E-mail: rudi.schaefer@physik.uni-marburg.de

1. Introduction

The stability of quantum systems under perturbation of the dynamics has attracted a considerable amount of attention in recent years. From a practical point of view this was motivated by a surge of activity in quantum information, where this question is crucial; from a more abstract point of view the implications for “quantum chaos” have been studied [1]. Fidelity, as a measure for this stability, has become a standard benchmark for the reliability of quantum information processing [2]. Following reference [3], we shall consider two unitary operators $U'(t)$ and $U(t)$ for the perturbed and unperturbed time evolution, respectively. The fidelity amplitude for some initial state $\psi(0)$ is defined as

$$f(t) = \langle \psi(0) | U^\dagger(t) U'(t) | \psi(0) \rangle \quad (1)$$

and the fidelity by $F(t) = |f(t)|^2$. In other words, the fidelity amplitude is the cross-correlation function of an initial state $\psi(0)$ evolving under two different dynamics, namely $U(t)$ and $U'(t)$. It can be reinterpreted as the autocorrelation function of the same initial state evolving under the echo operator $M(t) = U^\dagger(t) U'(t)$ which propagates the system forward and backward in time.

The reason why the fidelity or fidelity amplitude are so attractive is that it gives a measure of the average sensitivity to perturbations. In quantum optics there are proposals for experiments to measure directly the fidelity amplitude. The idea is to study the centre of mass motion of a two level atom in a potential being slightly different for the first and the second level. Preparing the atom in a superposition of the two levels and measuring the decay of the off-diagonal matrix element of the 2×2 density matrix, one obtains the fidelity amplitude of the center of mass motion of the atom in the external potential [4, 5, 6].

The motivation for the present work comes from recent fidelity studies using microwaves [7] and elastic waves [8]. In both types of experiments the waves are coupled to the systems by means of antennas or transducers, and reflection or transmission measurements are performed. The antennas correspond to external channels, i.e. scattering theory is needed to interpret the experiments. It thus becomes evident that a generalized concept of fidelity is called for based on the elements of the scattering matrix.

To study the sensitivity of the S-matrix to perturbations we therefore propose to define the scattering fidelity of an S-matrix element as the cross-correlation function of a matrix element of a perturbed and an unperturbed S-matrix taken in the time-domain and normalized by the corresponding autocorrelation functions. We shall see that this adequately describes the experimental situation, by presenting an experiment with two flat microwave cavities, both chaotic but one with and one without bouncing-ball states.

We show that scattering fidelity is equivalent to the fidelity amplitude (1) for chaotic dynamics and weak coupling; in that case furthermore all scattering fidelities are equivalent and we therefore can improve averages by averaging over channels. The possibility to replace or improve ensemble averages for S-matrix elements was

theoretically discussed in reference [9] and applied in reference [10] to evaluate the distribution of absolute values of diagonal and off-diagonal S-matrix elements in a problem with many open channels. We then compare the results of our experiment with the result for a random matrix model developed in [11]. Indeed the experimental results are reproduced without a fit parameter if the somewhat tedious task is carried out to determine the strength of the perturbation independently from level dynamics.

In the next section we define scattering fidelity and its weak coupling limit, then we describe the experimental setup (section 3). In section 4 we present a semi-classical evaluation of the perturbation strength for our setup, followed by a presentation of the experimental results and a comparison with random matrix theory (section 5). Particular attention is paid to the effect of bouncing ball states. In the conclusions (section 6), we discuss situations where we expect the scattering fidelity to differ from the fidelity amplitude, and we consider possible experiments.

2. Scattering fidelity

Here, we analyse the stability of a scattering system under perturbation of the Hamiltonian. This leads us to the definition of the scattering fidelity for individual matrix elements of the scattering matrix. Once the new quantity is defined, we ask, under which circumstances that quantity approximates the standard fidelity, equation (1).

Consider a scattering system which can be perturbed in a controlled way, e.g. by changing an external parameter. Suppose $S'(E)$ and $S(E)$ are the scattering matrices corresponding to the perturbed and unperturbed system, respectively. We denote a cross-correlation function of two scattering matrix elements by

$$C[S_{ab}^*, S'_{cd}](E) = \langle S_{ab}^*(E') S'_{cd}(E' + E) \rangle - \langle S_{ab}^*(E') \rangle \langle S'_{cd}(E' + E) \rangle, \quad (2)$$

where the brackets denote an energy window and/or an ensemble average. Even though the scattering matrix is defined in terms of stationary solutions to a dynamical system, we may use its Fourier transform $\hat{S}(t)$, to obtain a time dependent quantity. Due to the convolution theorem [12] such correlation functions are natural candidates for the construction of an open systems' analogue to the fidelity amplitude.

$$\hat{C}[S_{ab}^*, S'_{ab}](t) = \int dE e^{2\pi i Et} C[S_{ab}^*, S'_{ab}](E) \propto \langle \hat{S}_{ab}(t)^* \hat{S}'_{ab}(t) \rangle. \quad (3)$$

This quantity is dominated by the decay of the autocorrelations, and we therefore include a normalization into the definition of the scattering fidelity amplitude:

$$f_{ab}(t) = \frac{\langle \hat{S}_{ab}(t)^* \hat{S}'_{ab}(t) \rangle}{\sqrt{\langle |\hat{S}_{ab}(t)|^2 \rangle \langle |\hat{S}'_{ab}(t)|^2 \rangle}}. \quad (4)$$

Note that a spectral average taken in equation (2), is equivalent to an appropriate smoothing of the time signals (see reference [8]).

In what follows, we assume that the scattering system can be described by the effective Hamiltonian approach [18]. Then, for chaotic systems it holds that the

definition (4) approaches the usual fidelity amplitude in the weak-coupling limit. To show that, we consider the following parametrization of the scattering matrix

$$S_{ab}(E) = \delta_{ab} - i V^{(a)\dagger} \frac{1}{E - H_{\text{eff}}} V^{(b)} \quad H_{\text{eff}} = H_{\text{int}} - (i/2) [V V^\dagger + \Gamma_W] , \quad (5)$$

where $V^{(a)}$ is the column vector of V corresponding to the scattering channel a . For later use, we introduce the absorption width Γ_W , which is simply a scalar in the present context. This is equivalent to model absorption with infinitely many perturbatively coupled channels, whose partial widths add up to Γ_W [19].

Consider two slightly different Hamiltonians $H_{\text{int}} = H_{\text{int}}(\lambda_1)$ and $H'_{\text{int}} = H_{\text{int}}(\lambda_2)$, and the corresponding S-matrices as defined in (5) and denoted by S_{ab} and S'_{ab} . The Fourier transform of S'_{ab} reads:

$$\hat{S}'_{ab}(t) = -i \int dE e^{-2\pi i E t} V^{(a)\dagger} \frac{1}{E - H'_{\text{eff}}} V^{(b)} = -2\pi \theta(t) V^{(a)\dagger} e^{-2\pi i H'_{\text{eff}} t} V^{(b)} , \quad (6)$$

and similarly for S_{ab} . Here, $\theta(t)$ is the Heaviside function. The effective Hamiltonians H'_{eff} and H_{eff} differ only in their Hermitian part which is H'_{int} or H_{int} , respectively. Without restricting generality (otherwise, we must perform an Engelbrecht-Weidenmüller transformation [13]), we may assume that $V = \sum_c \sqrt{w_c} |v_c\rangle$, where $|v_1\rangle, \dots, |v_M\rangle$ are ortho-normal vectors in the Hilbert space of the closed system. For the product of two Fourier transformed S-matrix elements, as needed in equation (3), we get:

$$\hat{S}_{ab}(t)^* \hat{S}'_{ab}(t) = 4\pi^2 \theta(t) w_a w_b e^{-2\pi \Gamma_W t} \langle v_b | e^{2\pi i H_{\text{int}} t - \pi V V^\dagger t} | v_a \rangle \langle v_a | e^{-2\pi i H'_{\text{int}} t - \pi V V^\dagger t} | v_b \rangle . \quad (7)$$

The most unpleasant difference to the usual definition of a fidelity amplitude is the projector $|v_a\rangle \langle v_a|$ between forward and backward propagation. However, under chaotic dynamics, and if $|v_a\rangle$ and $|v_b\rangle$ are statistically independent, the energy/ensemble average converts that projector into the unit matrix (multiplied by $1/L$). We then obtain:

$$\left\langle \hat{S}_{ab}(t)^* \hat{S}'_{ab}(t) \right\rangle = \frac{4\pi^2}{L} \theta(t) w_a w_b e^{-2\pi \Gamma_W t} \langle v_b | U_{\text{eff}}^\dagger(t) U'_{\text{eff}}(t) | v_b \rangle , \quad (8)$$

where $U_{\text{eff}}(t)$ and $U'_{\text{eff}}(t)$ are the sub-unitary propagators for the respective internal Hamiltonians with channel coupling. This looks formally like a fidelity amplitude for the effective Hamiltonians of the system. However, even without any perturbation, this quantity is not constant, but yields the autocorrelation function (i.e. the power spectrum). This is the motivation to define the *scattering fidelity* f_{ab} for both diagonal and off-diagonal S-matrix elements via the relation

$$\left\langle \hat{S}_{ab}(t)^* \hat{S}'_{ab}(t) \right\rangle = f_{ab}(t) \left\langle |\hat{S}_{ab}(t)|^2 \right\rangle , \quad (9)$$

or, more symmetrically, by equation (4).

In the limit of weak coupling to the antennas, the scattering fidelity $f_{ab}(t)$ approaches the fidelity of the closed system. More rigorously, it must be required that the time scale for decay associated to the coupling $V V^\dagger$ is small as compared to the time

scale for the decay of the scattering fidelity. In this case the wall absorption, described by Γ_W , is the only remaining effect leading to:

$$\left\langle \hat{S}_{ab}(t)^* \hat{S}'_{ab}(t) \right\rangle \sim \frac{4\pi^2}{L} \theta(t) w_a w_b e^{-2\pi\Gamma_W t} f(t) \sim f(t) \left\langle |\hat{S}_{ab}(t)|^2 \right\rangle, \quad (10)$$

where $f(t)$ is the fidelity amplitude of the closed system with respect to the initial state $|v_b\rangle$. This argumentation assumes that $|v_a\rangle$ and $|v_b\rangle$ are statistically independent, in particular $a \neq b$. The result holds, however, for the case $a = b$ as well, provided that $|v_a\rangle$ is effectively a random state in the eigenbasis of H_{int} .

For chaotic dynamics, we have shown that in the limit of small antenna coupling, the scattering fidelity $f_{ab}(t)$ approaches the fidelity of the closed system. In this case, there is no restriction on the strength of the perturbation. However, an alternative derivation may be based on the rescaled Breit-Wigner approximation [20, 19]. That line of argument is presented in Appendix A. It is valid in the perturbative regime, only, but permits larger antenna couplings (as long as the rescaled Breit-Wigner approximation remains valid). The experimental results presented below have been obtained in either one of these regimes.

3. Experimental setup

Since a detailed description of the general experimental technique can be found e.g. in [17], we concentrate on the aspects relevant in the present context. Reflection and transmission measurements have been performed in a flat microwave cavity, with top and bottom plate parallel to each other. The cavity is quasi-two-dimensional for frequencies $\nu < \nu_{\text{max}} = c/(2h)$, where h is the height of the billiard. In this regime there is a complete equivalence between the stationary wave equation and the corresponding stationary Schrödinger equation, where the z component of the electric field corresponds to the quantum mechanical wave function,

$$(\Delta + E) \Psi(x, y) = 0, \quad E = \left(\frac{2\pi\nu}{c} \right)^2, \quad (11)$$

with Dirichlet boundary conditions.

To describe the experiments adequately, it is essential to take into account that the microwave system is in fact an open system. The microwave field in the cavity is constantly fed via one antenna, while the second antenna and, most importantly, the non-ideal cavity walls act as sinks. Scattering theory, originally developed in nuclear physics [18], can be applied directly to open microwave billiards as well [14], if absorption is properly taken into account [19]. With H_{int} being the Hamiltonian of the closed billiard, and two antennas projecting into the resonator at the positions \vec{r}_1 and \vec{r}_2 , the scattering matrix is precisely of the form given in equation (5). In the present context, $V^{(a)}$ corresponds to the antenna at position \vec{r}_a . For antenna diameters small compared to the wavelength the matrix elements V_{ja} are proportional to $\psi_j(\vec{r}_a)$, the wave functions of the unperturbed system at the antenna positions. Absorption is included by adding the width Γ_W (as a scalar) to the imaginary part of H_{eff} .

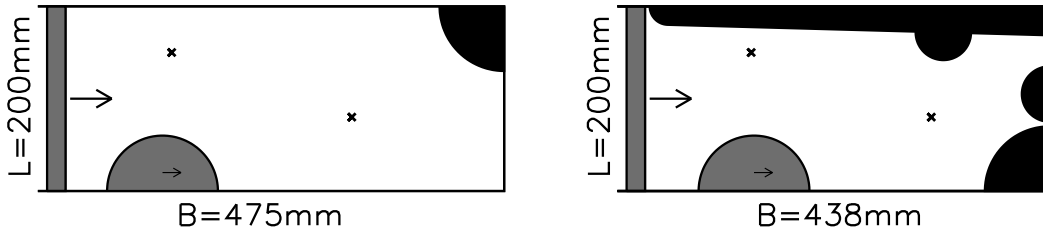


Figure 1. Geometry of the billiards. In the right billiard bouncing balls have been avoided by inserting additional elements (see text for dimensions).

Both antennas consisted of copper wires with a diameter of 1 mm, projecting 3 mm into the resonator; their positions in the billiard were fixed for all measurements. An Agilent 8720ES vector network analyzer was used to determine the complete S-matrix. Measurements were taken in the frequency range from 3 to 17 GHz with a resolution of 0.5 MHz.

The geometries of the billiards studied in this paper are shown in figure 1. One billiard consists of a rectangular cavity of length $L = 475$ mm, width $B = 200$ mm and height $h = 8$ mm, a quarter-circle insert of radius $R_1 = 70$ mm, and a half-circle insert of radius $R_2 = 60$ mm placed at the lower boundary. The position of the latter was changed in steps of 20 mm to get 15 different systems for the ensemble average. The perturbation of the system was achieved by moving the left wall in steps of 0.2 mm. For each of the 15 positions of the half-circle we performed 11 measurements for different perturbation strengths.

The other billiard consists of the same rectangular cavity, but with length $L = 438$ mm. It also shares the quarter-circle insert of radius $R_1 = 70$ mm, and on the lower boundary the half-circle insert of radius $R_2 = 60$ mm, which again was moved to realize an ensemble of 15 systems. Additional elements were inserted into the billiard to avoid bouncing-ball resonances: two half-circle inserts with radius $R_3 = 30$ mm, and a wedge on the upper boundary. Again the perturbation of the system was realized by moving the left wall in 10 steps of 0.2 mm.

The classical dynamics for the geometry of the billiards is dominantly chaotic, and since these are time-reversal invariant systems, we are going to compare the experimental results with random matrix predictions for the Gaussian orthogonal ensemble.

4. Perturbation parameter for shifting of a billiard wall

In billiard systems the parameter variation is not due to a change of the Hamiltonian, but of the boundary condition. It was shown in chapter 5 of reference [14] that both situations are equivalent for the case that the parameter variation in the billiard is due to a shift of a straight wall. In this case the matrix element of the equivalent perturbation

is given by

$$(H_1)_{nm} = l \int_0^L \frac{\partial \psi_n(0, y)}{\partial x} \frac{\partial \psi_m(0, y)}{\partial x} dy, \quad (12)$$

where l is the shift of the wall (in x -direction) and L is the length of the shifted wall. It follows for the perturbation strength:

$$\begin{aligned} \lambda^2 &= \langle [(H_1)_{nm}]^2 \rangle \\ &= l^2 \int_0^L dy_1 \int_0^L dy_2 \left\langle \frac{\partial \psi_n(0, y_1)}{\partial x} \frac{\partial \psi_n(0, y_2)}{\partial x} \right\rangle \left\langle \frac{\partial \psi_m(0, y_1)}{\partial x} \frac{\partial \psi_m(0, y_2)}{\partial x} \right\rangle \end{aligned} \quad (13)$$

This is true for $n \neq m$, but again the result can be easily generalized to the case $n = m$. The averages can be calculated by means of Berry's conjecture of the superposition of random plane waves [21]. Close to a straight wall with Dirichlet boundary conditions, this yields

$$\begin{aligned} &\langle \psi_n(x_1, y_1) \psi_n(x_2, y_2) \rangle \\ &= \frac{1}{A} \left[J_0 \left(k \sqrt{(x_1 - x_2)^2 + (y_1 - y_2)^2} \right) - J_0 \left(k \sqrt{(x_1 + x_2)^2 + (y_1 - y_2)^2} \right) \right] \end{aligned} \quad (14)$$

for the spacial correlation function, where A is the billiard area. Inserting this into equation (13) we obtain for the case $n \neq m$:

$$\begin{aligned} \lambda^2 &= \langle [(H_1)_{nm}]^2 \rangle \\ &= \frac{4k^2 l^2}{A^2} \int_0^L dy_1 \int_0^L dy_2 \frac{1}{(y_1 - y_2)^2} [J'_0(k|y_1 - y_2|)]^2 \\ &= \frac{4k^2 l^2}{A^2} \int_0^L dy_1 \int_{-y_1}^{L-y_1} dy_2 \frac{1}{y_2^2} [J'_0(ky_2)]^2 \\ &\approx \frac{4k^2 l^2}{A^2} \int_0^L dy_1 \int_{-\infty}^{\infty} dy \frac{1}{y^2} [J'_0(y)]^2 \\ &= \frac{4k^2 l^2 L}{A^2} \frac{8}{3\pi} \end{aligned}$$

The approximation works well for large wave numbers k . Since the mean level distance is normalized to one, we can insert $A = 4\pi$ for the area of the billiard, and finally end up with:

$$\lambda^2 = \frac{2L}{3\pi^3} k^3 l^2 \quad (15)$$

The variance of the diagonal matrix elements, $\langle [(H_1)_{nn}]^2 \rangle$, yields a value twice as large. Exactly the same expression was obtained by Lebœuf and Sieber in a completely different approach [22] using periodic orbit theory and the ergodicity assumption. It is interesting to note that two seemingly unrelated assumptions, one on the Gaussian distribution of wave function amplitudes, and the other on the ergodicity of long periodic orbits, yield identical results.

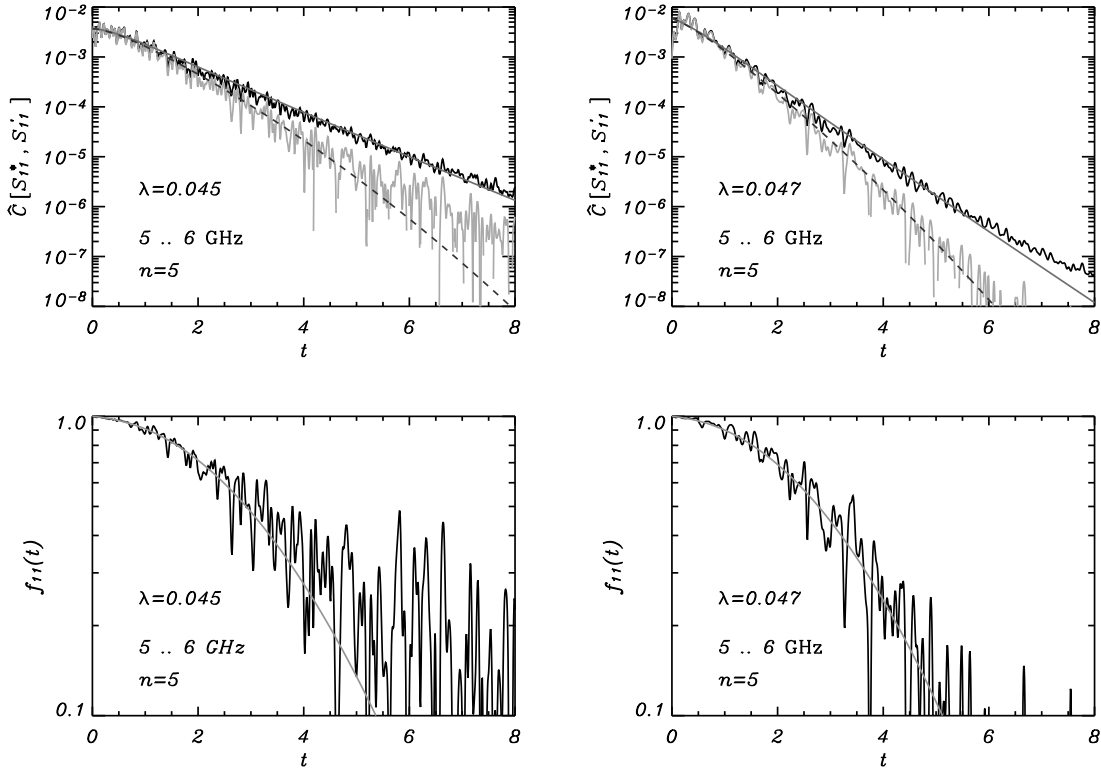


Figure 2. (top): Logarithmic plot of the correlation function $\hat{C}[S_{11}^*, S_{11}']$ for the billiard with bouncing balls (left), and for the one without bouncing-balls (right). The experimental results for the autocorrelation are shown in black, while the correlation of perturbed and unperturbed system are shown in grey. The smooth solid curve corresponds to the theoretical autocorrelation function, and the dashed curve to the product of autocorrelation function and fidelity amplitude.

(bottom): Logarithmic plot of the corresponding fidelity amplitudes. The smooth curve shows the linear-response result. For the billiard without bouncing balls the perturbation parameter λ was obtained from the variance of the level velocities; in the other case it was fitted to the experimental curve.

5. Experimental results

5.1. Correlation function and fidelity amplitude

We start with a discussion of the Fourier transform of the correlation function $\hat{C}[S_{11}^*, S_{11}'](t)$ as given in equation (3). Figure 2 shows a logarithmic plot of $\hat{C}[S_{11}^*, S_{11}'](t)$ in comparison to the autocorrelation function $\hat{C}[S_{11}^*, S_{11}](t)$. The change of area and surface due to the perturbation, i. e. the shift of the billiard wall, was taken into account by unfolding the spectra to a mean level distance of one. The frequency window of the Fourier transforms was 1 GHz wide, and a Welch filter was applied. The correlation functions were averaged over an ensemble of 15 billiard geometries.

The autocorrelation follows the corresponding theoretical curve nicely, where the parameters for the wall absorption and the coupling of the antennas had been determined

as described in reference [19]. Minor deviations from the theoretical curve can be attributed to the small number of levels in this frequency interval. Furthermore, small slits between the inserts of the billiards may act as additional decay channels. This is in contrast to the more or less homogenous absorption by the cavity wall, which can be described by infinitely many weak channels [19].

With increasing time, the correlation function $\hat{C}[S_{11}^*, S'_{11}](t)$ deviates more and more from the autocorrelation function. This behaviour can be described by a product of the autocorrelation function and the fidelity amplitude $f(t)$ of the closed system, thus confirming expression (10).

As an expression for the fidelity amplitude, we use the one derived by Gorin et al. [11] based on the linear-response approximation,

$$f(t) = e^{-4\pi^2\lambda^2 C(t)}. \quad (16)$$

For the Gaussian orthogonal ensemble $C(t)$ is given by

$$C(t) = t^2 + \frac{t}{2} - \int_0^t \int_0^\tau b_2(\tau') d\tau' d\tau, \quad (17)$$

where $b_2(t)$ is the two-point form factor. Equation (16) describes the fidelity amplitude both in the perturbative regime, where the Gaussian decay is dominant, and in the Fermi golden rule regime, which shows an initial exponential decay.

In the following we shall study the fidelity amplitude directly as the deviation from the autocorrelation function as defined in equation (4) to achieve a more direct comparison with theory. There are two reasons for dividing by the experimental autocorrelation function: there is no need to fit the autocorrelation function, and the influence of non-generic features in the Fourier transform is reduced.

The plots in the lower row of figure 2 show that this procedure works very well. For the billiard without bouncing balls and the frequency range shown in this figure, the perturbation strength was determined directly from the measured spectra via the variance of the level velocities. Thus we can describe the experimental results for the fidelity amplitude by the linear-response expression without any free parameter.

As expected, the billiard with bouncing balls shows systematic deviations from the random matrix prediction. Only for small times t we find good agreement. We therefore concentrate on the results of the billiard without bouncing balls in the following subsections.

5.2. Agreement with the linear-response prediction

In our experiment the values for the perturbation parameter λ vary from $\lambda = 0.01$ for $n = 1$ and $\nu = 3.4$ GHz up to $\lambda = 0.5$ for $n = 10$ and $\nu = 17 \dots 18$ GHz. Figure 3 shows the fidelity amplitude for four different frequency windows. The perturbation parameter λ has been fitted to the experimental curves. To improve statistics, experimental results for f_{11} , f_{22} and f_{12} have been superimposed. The individual curves for these quantities were not discernible within the limit of error.

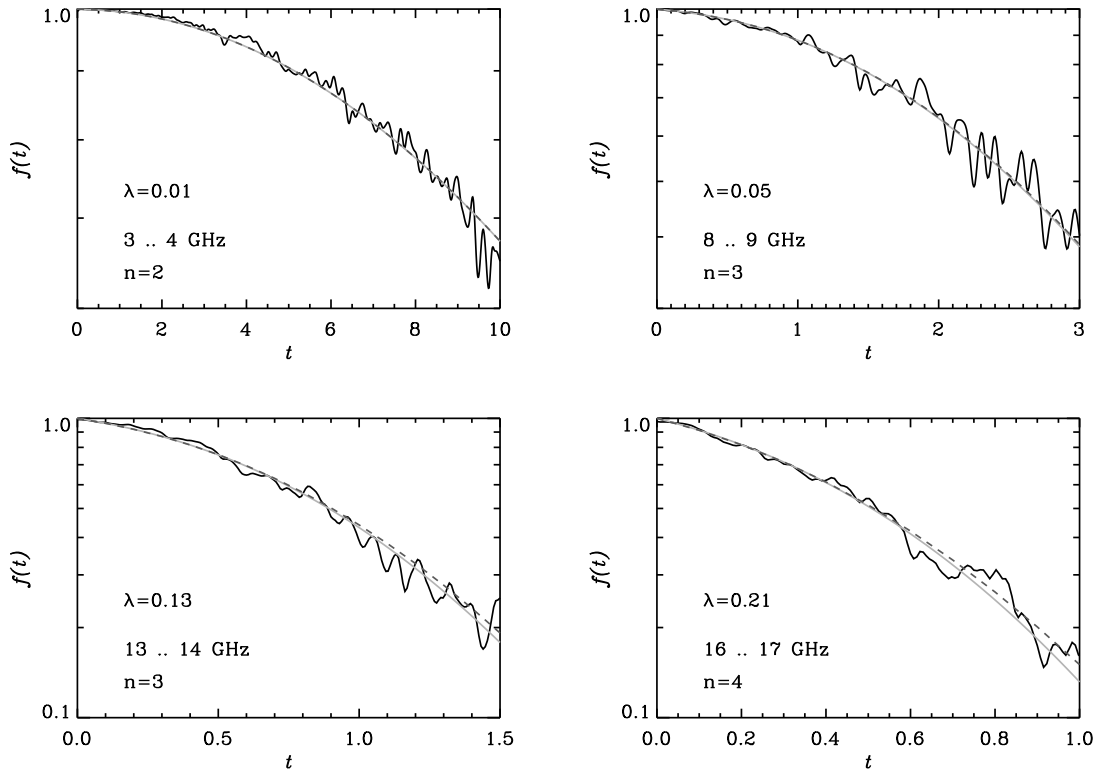


Figure 3. Fidelity amplitude of the billiard without bouncing balls, obtained by superimposing results for f_{11} , f_{22} and f_{12} . The smooth solid line shows the linear-response result (16), while the dashed line shows the exact result [15]. The perturbation parameter λ_{exp} has been fitted to each experimental curve.

For small perturbation strengths, the linear term in the exponential is still close to one and thus we observe essentially a Gaussian decay of the fidelity amplitude, as seen in figure 3 for $\lambda_{\text{exp}} = 0.01$. With increasing perturbation strength the linear term is getting more pronounced, leading to an exponential decay for small times. However, for larger times the Gaussian decay again becomes dominant.

In the range accessible to our experiment (limited by the small ensemble) we find good agreement with the linear-response prediction of the random matrix model. For the strongest perturbation strength realized in our experiment, deviations of the linear-response result from the exact result for the Gaussian ensemble [15] become noticeable only at times where $f(t)$ has decayed already below 10^{-1} . These deviations could not be detected by our experiment.

In [8] Lobkis and Weaver report on a very similar experiment in elastodynamic billiards. There, the principal quantity of interest is called distortion, denoted by $D(t)$. In our terminology, it is the logarithm of the scattering fidelity: $D(t) = -\ln f_{aa}(t)$. Interestingly, the experiment itself is performed in the time domain. A short acoustic pulse is coupled into the sample via a pointlike pin transducer, and with the same device the time signal corresponding to the response of the system is measured. Cross-

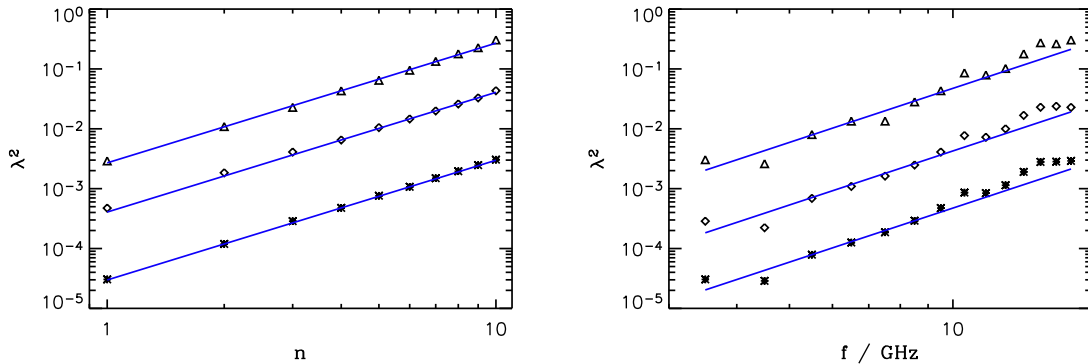


Figure 4. Perturbation strength λ^2 as a function of n (left), and as a function of frequency ν (right). The slopes of the straight lines are 2 in the left, and 3 in the right hand figure. The results are shown for the billiard without bouncing balls.

correlating two such signals, measured at slightly different temperature allows to extract the scattering fidelity, where the perturbation is due to the temperature change. In [16] the experimental data from [8] are reanalyzed, showing again an excellent agreement with the random matrix prediction, derived in [11].

5.3. Scaling behavior of the perturbation strength

The experimental fidelity amplitude was studied for 10 different shifts of the billiard wall ($\Delta l = n \cdot 0.2$ mm, with $n = 1 \dots 10$), and a frequency window of width 1 GHz was moved through the spectrum. The perturbation strength λ^2 entering the fidelity amplitude (16) was fitted to the experimental results.

Figure 4(a) shows the experimental perturbation strength λ_{exp}^2 in dependence of the number of steps n for three different frequency regimes. We observe an excellent agreement with the scaling $\lambda^2 \propto n^2$ as predicted from equation (15). The experimental results for λ_{exp}^2 in dependence of the frequency range are shown in figure 4(b). They do not look quite as nice as the previous results, but they still confirm the scaling $\lambda^2 \propto \nu^3$.

In view of the good agreement with the predicted scaling of the perturbation strength, we can now test the time dependence implied by $C(t)$ with better statistics by averaging over all data after rescaling: In figure 5, these averages are plotted against $4\pi^2\lambda^2 C(t)$ and we see that the linear response solution of the random matrix model [11] describes all data very well. However, the slope of the resulting curve is not in accordance with the prediction and yields a λ_{exp}^2 deviating from the theoretical expectation of equation (15) by a factor of 0.36.

This deviation is caused by the fact that we are far from the semi-classical limit, for which the expression for λ^2 was derived. This is in accordance with numerical calculations for the Sinai billiard done by H. Schanz in Göttingen [23]. In cases where we determined the variance of level velocities directly from the measured spectra, we found the same deviation from equation (15). This shows that the experiment can be

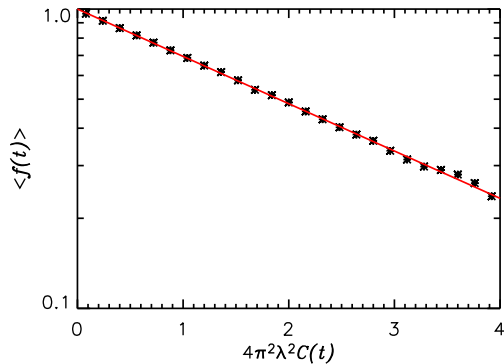


Figure 5. Average of the experimental fidelity amplitude on a rescaled axis $x = 4\pi^2\lambda^2 C(t)$. The solid line corresponds to $g(x) = \exp(-\alpha x)$ with $\alpha = \lambda_{\text{exp}}^2/\lambda^2 = 0.36$.

described in a self-consistent way.

5.4. Influence of bouncing-ball modes

To study the frequency dependence of the perturbation strength in some more detail, we took a smaller frequency window of 0.5 GHz for the Fourier transform and moved it in finer steps through the whole frequency range.

In Figure 6 the ratio $\lambda_{\text{exp}}^2/\lambda^2$ is plotted both for the billiard with and without bouncing balls, where λ^2 is the theoretical value of the perturbation strength according to equation (15).

In the right hand plot, the frequencies of the vertical bouncing ball resonances are plotted as vertical lines, revealing the origin of the peaks in the frequency dependence of λ_{exp}^2 . The vertical bouncing ball states correspond to standing waves between the long sides of the billiard and remain nearly unaffected by the perturbation. However, the unfolding of each spectrum takes the change of area into account, and thus introduces a constant drift to these resonances. This leads to a faster decay of the fidelity, thus resulting in the strong peaks visible in the figure.

Note that the result for the billiard without bouncing balls still shows fluctuations. The influence of the eigenmodes in the individual frequency window is thus visible for this billiard as well. However, there are no systematic peaks like the ones for the bouncing-ball modes.

6. Conclusions

It was shown in this paper that the scattering fidelity $f_{ab}(t)$ is an easily accessible quantity which in the weak-coupling limit approaches the ordinary fidelity amplitude $f(t)$. It is stressed that it is not necessary to vary the antenna position for this purpose. For integrable systems, however, an average over the antenna positions is indispensable to obtain $f(t)$. Therefore a determination of the fidelity $f(t)$ from the scattering fidelity

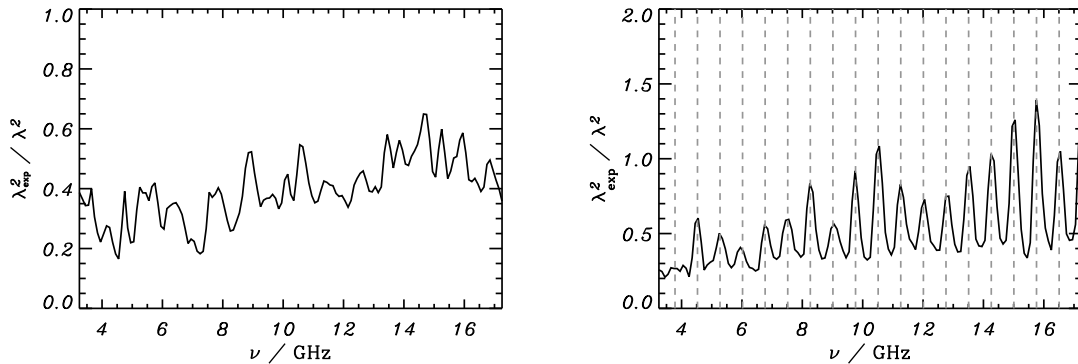


Figure 6. $\lambda_{\text{exp}}^2/\lambda^2$ as a function of frequency ν . Results for the billiard without (left) and with bouncing balls (right). The dashed lines correspond to the eigenfrequencies of the associated bouncing-ball states.

$f_{ab}(t)$ as illustrated here, is probably not feasible in that case.

All results of the present paper could be described within the limits of the exponentiated linear-response approximation [11], allowing a nice scaling of all data onto one single curve. Deviations of the decay constant of the such scaled fidelity from the predicted value could be quantitatively traced back to limits of the semiclassical approximation.

A general perturbation of the scattering matrix, is not necessarily restricted to the internal dynamics, as it may also change the coupling to the channels. For practical reasons, the present experimental setup was not well suited to study such a situation, and we are planning a further experiment to study scattering fidelity as a function of coupling strength.

Acknowledgments

T Prosen, U Kuhl and H Schanz are thanked for helpful discussions taking place in part on occasion of a workshop at the Centro Internacional de Ciencias in Cuernavaca, Mexico. We thank R L Weaver for drawing our attention to reference [8]. The experiments were supported by the Deutsche Forschungsgemeinschaft, and T. H. S. acknowledges support under grants CONACyT # 41000-F and UNAM-DGAPA IN-101603.

Appendix A. Scattering fidelity in the rescaled Breit-Wigner approximation

We assume that the spectrum of the unperturbed closed system (Hamiltonian H_{int}) may be taken from the Gaussian orthogonal ensemble (GOE), and consider averages over that ensemble. In the rescaled Breit-Wigner approximation [20], the correlation

function (7) reads

$$\begin{aligned} \left\langle \hat{S}_{ab}(t)^* \hat{S}'_{ab}(t) \right\rangle &= 4\pi^2 \theta(t) \left\langle \sum_{jk} \langle a|V|j\rangle \langle j| e^{2\pi i(E_j + i\Gamma_j/2)t} |j\rangle \langle j|V|b\rangle \right. \\ &\quad \left. \times \langle b|V|k'\rangle \langle k'| e^{2\pi i(E'_j - i\Gamma'_j/2)t} |k'\rangle \langle k'|V|a\rangle \right\rangle, \end{aligned} \quad (\text{A.1})$$

where we have used Dirac's notation for the eigenbases $\sum_j |j\rangle \langle j|$ and $\sum_k |k'\rangle \langle k'|$ of H_{int} and H'_{int} , respectively. The numbers Γ_j and Γ'_j denote the diagonal element of the anti-Hermitian part of H_{eff} and H'_{eff} in the respective basis. We will relate this correlation function to the fidelity amplitude of the closed system H_{int} , or H'_{int} (when perturbed). To this end, we need to restrict ourselves to the perturbative regime. In this case, $|j'\rangle = |j\rangle$ and $\Gamma'_j = \Gamma_j$, so that

$$\begin{aligned} \left\langle \hat{S}_{ab}(t)^* \hat{S}'_{ab}(t) \right\rangle &= 4\pi^2 \theta(t) \sum_{jk} \left\langle V_{ja}^* V_{jb} V_{kb}^* V_{ka} e^{-\pi(\Gamma_j + \Gamma_k)t} e^{-2\pi i(E'_k - E_j)t} \right\rangle \\ &= \sum_k \left\langle e^{-2\pi i(E'_k - E_k)t} \right\rangle \sum_j \left\langle V_{ja}^* V_{jb} V_{kb}^* V_{ka} e^{-\pi(\Gamma_j + \Gamma_k)t} e^{-2\pi i(E_k - E_j)t} \right\rangle. \end{aligned} \quad (\text{A.2})$$

The separation of averages in the second line is possible in the perturbative regime, only. There $E'_k - E_k$ is just the diagonal element of the perturbation matrix and hence statistically independent of the unperturbed system. The average $\langle \exp[-2\pi i(E'_k - E_k)t] \rangle$ gives the fidelity amplitude, independent of the index k , while the rest is just the autocorrelation function of the S-matrix element S_{ab} .

$$\left\langle \hat{S}_{ab}(t)^* \hat{S}'_{ab}(t) \right\rangle = f(t) \left\langle |\hat{S}_{ab}(t)|^2 \right\rangle. \quad (\text{A.3})$$

References

- [1] Peres A 1984 *Phys. Rev. A* **30** 1610
- [2] Nielsen M A and Chuang I L 2000 *Quantum Computation and Quantum Information* (Cambridge, Cambridge University Press)
- [3] Prosen T, Seligman T H and Žnidarič M 2003 *Prog. Theor. Phys. Suppl.* **150** 200
- [4] Gorin T, Prosen T, Seligman T H and Strunz W T 2004 *Phys. Rev. A* **70** 042105
- [5] Gardiner S A, Cirac J I and Zoller P 1997 *Phys. Rev. Lett.* **79** 4790
- [6] Haug F, Bienert M, Schleich W P, Seligman T H and Raizen M G 2005 *Phys. Rev. A* **71** 043803
- [7] Schäfer R, Stöckmann H-J, Gorin T and Seligman T H 2004 *nlin.CD/0412053*
- [8] Lobkis O I and Weaver R L 2003 *Phys. Rev. Lett.* **90** 254302
- [9] Nemes M C and Seligman T H 1980 *Z. Phys. A* **295** 243
- [10] Jung C and Seligman T H 1997 *Phys. Rep.* **285** 77
- [11] Gorin T, Prosen T and Seligman T H 2004 *New J. Phys.* **6** 20
- [12] Brigham E O 1974 *The Fast Fourier Transform* (New York: Prentice Hall)
- [13] Engelbrecht, C A and Weidenmüller H A 1973 *Phys. Rev. C* **8** 859
- [14] Stöckmann H J 1999 *Quantum Chaos - An Introduction* (Cambridge: University Press)
- [15] Stöckmann H J and Schäfer R 2004 *New J. Phys.* **6** 199
Stöckmann H J and Schäfer R 2004 *nlin.CD/0409021*
- [16] Gorin T, Seligman T H and Weaver R L 2005 unpublished

- [17] Kuhl U, Persson E, Barth M and Stöckmann H J 2000 *Eur. Phys. J. B* **17** 253
- [18] Mahaux C and Weidenmüller H A 1969 *Shell-Model Approach to Nuclear Reactions* (Amsterdam: North-Holland)
- [19] Schäfer R, Gorin T, Seligman T H and Stöckmann H J 2003 *J. Phys. A* **36** 3289
- [20] Gorin T and Seligman T H 2002 *Phys. Rev. E* **65** 026214
- [21] Berry M V 1977 *J. Phys. A* **10** 2083
Berry M V 2002 *J. Phys. A* **35** 3025
- [22] Lebœuf P and Sieber M 1999 *Phys. Rev. E* **60** 3969
- [23] Schanz H 2004 *Private communication*